Red mullet stock identification without any reference using otolith shape

Nicolas Andrialovanirina, Émilie Poisson Caillault, Kélig Mahé

Red mullet stock identification without any reference using otolith shape

N. Andrialovanirina[1,2] É. Poisson Caillault[1] K. Mahé[2]

[1] Univ. Littoral Côte d'Opale, UR 4491, LISIC, F-62100 Calais, France
[2] IFREMER, Unité HMMN, 150 quai Gambetta, F-62321 Boulogne-sur-Mer, France

nicolas.andrialovanirina@ifremer.fr ; emilie.poisson@univ-littoral.fr ; kelig.mahe@ifremer.fr

Résumé

Dans le cadre d'une pêche durable, subissant un changement global, la connaissance préalable des limites géographiques de chaque population étudiée est requise. Dans cette étude, l'analyse automatique innovante de la forme tridimensionnelle (3D) des otolithes des rougets barbets de la Mer Méditerranée a été comparée à l'analyse conventionnelle en bidimensionnel (2D). Il a été conclu que cette nouvelle technique tridimensionnelle de la forme était plus précise pour délimiter le stock, que ce soit en utilisant une classification non supervisée ou supervisée.

Mots Clef

Clustering, classification, otolithe de poisson, 3D, harmoniques de Fourier, structure de population

Abstract

In the context of sustainable fishing, amidst global change, prior knowledge of the geographic boundaries of each studied population is required. In this study, innovative automated analysis of the three-dimensional (3D) shape of red mullet otoliths from the Mediterranean Sea was compared to conventional two-dimensional (2D) analysis. This new three-dimensional shape technique was found to be more accurate in delineating the stock, whether using unsupervised or supervised classification.

Keywords

Clustering, classification, fish otolith, 3D, Fourier harmonics, population structure.

1 Introduction

Stocks serve as the fundamental unit for assessing fishery resources and establishing sustainable exploitation levels [29]. Effective fishery management depends critically on accurately delineating fish stocks, which is a fundamental requirement for analysing the dynamics and structure of fishery management units [6]. Each distinct stock responds uniquely to fishing pressure and management interventions. Misidentifying stock units can result in suboptimal management outcomes, heightening the risks of overfishing and hampering sustainability efforts [2]. Various methods exist for defining fish stocks (see summary in [13, 6]), including genetic markers, natural indicators (such as parasites), growth rates, fatty acids in tissues, life history traits, external tags, and microchemistry. Among these, sagittal otolith shape and microchemistry have emerged as widely used proxies for stock identification across diverse fish species [13, 6].

Otoliths, also known as "ear stones", are incrementally grown calcified structures [9]. Their shape and size vary from species to species, playing a crucial role in fish balance and hearing [9]. As individual markers, otoliths can be used to study fish growth, migration, and population dynamics [6, 13], while they also offer valuable insights into fish stock structure. Otolith shape results from a complex interplay of environmental conditions, genetic heritage, and ontogenetic evolution [7, 35]. Variations in otolith shape between individuals can even distinguish between interspecific and intraspecific fish. Otoliths are metabolically inert structures, without post-deposition alteration or resorption [9]. Recent advancements in image analysis, processing, and freely available libraries have significantly bolstered the use of otoliths as powerful tools in fish research. Notably, otolith shape analysis offers distinct advantages over genetic analysis for stock identification, primarily due to its cost-effectiveness with fast and efficient analysis [6]. There are various methods for analysing the shape of otoliths. Fourier analysis stands as a prevalent method employed to represent otolith shape [13], providing a detailed analysis of its contours and features. Another valuable technique for analysing otolith shape is wavelet analysis [24, 16]. This method provides a localized frequency description of the shape, making it particularly adept at identifying localized features [16]. By capturing variations in shape at different scales, wavelet analysis offers insights into both global and fine-scale features of the otolith. Geometric analysis entails identifying specific points (landmarks) on the otolith that correspond to biological or structural features [16]. In contrast to landmark analysis, outline analysis focuses on capturing the entire outline of the otolith rather than specific landmarks. This approach provides a holistic view of the otolith shape and can be implemented using various methods, includ-

ing Fourier Harmonics and wavelet descriptors [16]. Outline analysis allows researchers to assess shape variation across the entire contour of the otolith, offering valuable insights into its morphological characteristics [16]. However, the primary method employed to describe and to compare otolith shape is standardised Elliptical Fourier Descriptors (EFDs) [13], which serve as a potential tool for describing and comparing two-dimensional (2D) shapes.

Typically, otolith shape is extracted from two-dimensional images [6]. This view is, however, incomplete, using only one plane projection of a three-dimensional (3D) object. Potential bias may therefore arise during 2D acquisition due to the object's position. With advancements in imaging technology, 3D shape analysis of otoliths has become feasible. This approach provides a more comprehensive representation of otolith shape compared to traditional 2D analysis. By capturing the spatial arrangement and curvature of the otolith in three dimensions, 3D shape analysis offers enhanced insights into its structural complexity and biological significance. This method unveils features not discernible in 2D analysis, thereby expanding our understanding of otolith morphology and its ecological implications. Existing research on 3D otoliths are primarily focused on: scanning and/or extracting otolith shape in three dimensions [40, 18, 19, 34, 25]; understanding the functional role and evolution of the inner-ear and otoliths, particularly concerning sound effects and equilibration (*i.e.* individual spatial location) [26, 37]. A recent study on the red mullet demonstrated that 3D analysis effectively addresses significant asymmetry in otolith shape originating from the inner-ear side (*i.e.* left versus right ear) that was not observed in 2D analysis from the same dataset [1].

After characterizing the otolith shapes, the subsequent step involves classification techniques to discriminate fish stocks. No paper in the recent literature mentions 3D automatic classification. In 2D, Principal Component Analysis (PCA) is used mainly as a dimensionality reduction preprocessing step [13, 6]. The principal components facilitate visualisation and classification of otoliths. Unsupervised approaches encompass Hierarchical Clustering [39] and K-means Clustering [15], while supervised methods include Linear Discriminant Analysis (LDA) [8], Random Forests [38], and Support Vector Machines (SVM) [33] and, recently, some Deep Neural Network for age estimation [3].

This article aims to apply automatic classification approaches on the same 2D and 3D dataset to define stock structure. The case study is the red mullet (*Mullus barbatus*), a main important commercial fish species in the Mediterranean Sea. Beyond the 2D conventional stock identification approaches based on otolith shape, additional unsupervised classification methods, including density-based and spectral clustering with recursive version, alongside supervised basic pattern matching as K-Nearest-Neighbors were used. Two objectives are studied: (1) the efficiency of 3D shape analysis compared with 2D analysis in stock delimitation, and (2) the efficiency of basic unsupervised and/or supervised classification methods for stock identification. This paper is divided into three main parts. Section 2 is the experimental protocol from data acquisition to classification. Section 3 shows the results followed by the discussion section.

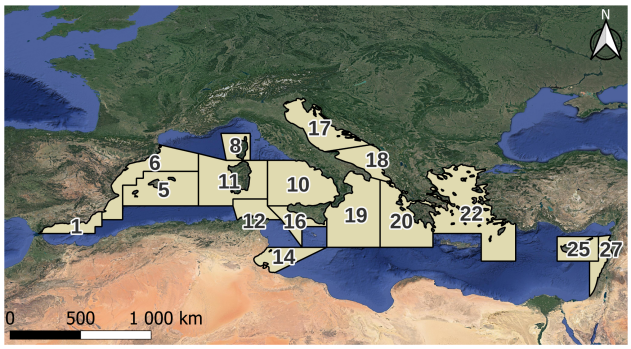

Figure 1: Segmentation of the Mediterranean Sea into the 16 geographical sub-areas (GSAs) used

2 Methodology

2.1 Sampling and label references

316 individual fish specimens were collected from 16 geographical sub-areas (GSAs), as defined by the General Fisheries Commission for the Mediterranean (GFCM). These GSAs represent diverse marine ecosystems within the Mediterranean Sea (see figure 1 and table 1). These

n^o GSA	2-stocks GFCM	3-stocks	n samples
1	1	1	7
5	1	1	23
6	1	1	12
8	1	1	12
10	1	1	13
11	1	1	5
12	1	1	19
14	1	1	16
16	1	2	58
17	1	2	8
18	2	2	30
20	2	2	20
22	2	2	36
23	2	3	18
25	2	3	24
27	2	3	27

Table 1: Sampling distribution by geographical sub-areas (GSAs) and proposal cuts of over fish stocks defined by expert groups [20, 21]

GFCM experts proposed two stocks described in table 1 based on other species' knowledge. The first proposal delimited 2 stocks according to 16-17 GSA boundaries [20]. The second proposed stock definition adds another stock built from 22-23 GSA [21]. The sampling campaign was

conducted during the 2019 international MEDiterranean International Trawl Survey (MEDITS survey), a substantial effort to assess fish populations and their habitats in the Mediterranean Sea [30]. The MEDITS survey provides a valuable dataset for understanding the distribution and characteristics of fish species. To ensure robustness in this analysis, potential ontogenetic effects on otolith shape are considered. Consequently, the sampling is restricted to young mature fishes (*i.e.* fish after their first sexual maturity and aged between 3 and 5 years old) within a total length range from 141 to 212 mm (with a mean length of 167±16 mm). Furthermore, only left otoliths (sagittae) are selected to avoid asymmetry factors. These choices ensure uniformity in our dataset and facilitate accurate comparisons across individuals. Environmental parameters have been integrated along side stock divisions (GSAs), using data extracted from models generated by the E.U. Copernicus Marine Service. Salinity, temperature, and velocity modules were derived from the Mediterranean Sea Physics Reanalysis (product identifier MEDSEA_MULTIYEAR_PHY_006_004) spanning from 1987 to 2019 [10]. These parameters were obtained from a grid with a horizontal resolution of 1/24° x 1/24° and 125 vertical levels, increasing in thickness with depth. The model assimilates satellite sea surface temperature and sea level, along with in-situ temperature-salinity profiles. Additionally, ten other variables were sourced from the Mediterranean Sea Biogeochemistry Reanalysis (product identifier MEDSEA_MULTIYEAR_BGC_006_008) covering the period from 1999 to 2019 [31]. These variables were acquired from a grid with the same horizontal resolution and vertical levels as the previous model. The biogeochemistry model assimilates satellite chlorophyll data and is driven by physical forcing fields from the Mediterranean physical model. Values relevant to the habitat of red mullet (typically found at depths between 20 and 300 meters) were extracted and summarized as median and range values (calculated as the difference between the third and first quantiles) across three temporal windows: 5 years (2014-2018), 3 years (2016-2018), and 1 year (2018). This was done based on the age range of the sampled red mullet (3-5 years; sampled in April 2019). Parameters exhibiting weak correlations (below 0.75) were retained for further analysis (table 2), the 1-year period year was selected due to the redundancy information.

Parameter Name	Feature (M/R)	Unit
Alkalinity	M/R	mol eq kg^{-1}
Chlorophyll concentration (as carbon)	M	mg(C) m^{-3}
Molar ammonium concentration	M	mmol m^{-3}
Molar nitrate concentration	M	mmol m^{-3}
Molar dissolved molecular oxygen concentration	M/R	mmol m^{-3}
pH	M	
Molar phosphate concentration	M/R	mmol m^{-3}
Net primary production of biomass per day	M	mg m^{-3} day^{-1}
Salinity	M	psu
Temperature	M	^{o}C
Velocity module	M	m s^{-1}

Table 2: Retained environmental parameters (M: Median, R: Range)

Leveraging these environmental parameters, a recursive spectral analysis [23] was conducted to generate division labels based on environmental conditions. Spectral recursive analysis stops the segmentation in 5 levels. Upon partitioning the environmental data using spectral recursive methodology, the initial division yielded two labels, while the final division resulted in seven labels (2).

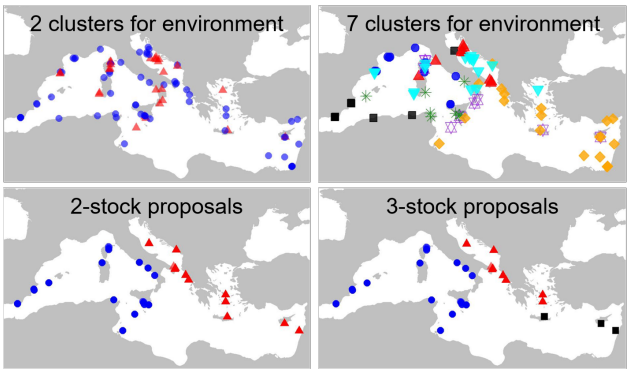

Figure 2: Delimitation by environmental data clustering and 2-stock or 3-stock units proposal by experts (groups are distinguished by a specific color and form)

2.2 Two-dimensional outlines and three-dimensional surfaces acquisition

Calibrated 2D images were taken using a binocular microscope (Leica MZ6) equipped with a 1.6x magnification and a SONY XCD-U100CR Camera. These images were captured under reflected light to reveal clear details of the otoliths. To ensure consistency in our otolith images, an R algorithm was developed to involve several essential steps. We carefully aligned all otoliths to ensure a consistent orientation. This step minimized any variations due to rotation or positioning. The grayscale otolith images were modified into binary representations, effectively creating black-and-white images. Binarization step simplified the shape representation and facilitated subsequent analyses. From the binarized images, we extracted the outlines that precisely represented the otolith shape. These outlines were used in the subsequent shape analysis. Otolith 3D images were acquired using an X-ray microtomograph. The process involved capturing two-dimensional X-ray images of the object at varied angles (covering a full rotation from 0° to 180°). These X-ray images revealed density disparities between the object and the surrounding air. We used the µCT Skyscan 1174 (Bruker). X-ray microtomograph

parameters included 800 µA intensity, 50 kV tube voltage (Tension) and 29.2 µm voxel size. After acquiring the X-ray images, the reconstruction of 3D images was performed using Nrecon software (Bruker). This process converted the X-ray images into a stack of virtual slices while preserving their spatial relationships. 3D Slicer facilitated segmentation, allowing us to extract the otolith isosurfaces as 3D meshes.

2.3 Two-dimensional and three-dimensional extraction of shape information

To ensure consistency, we selected a fixed number of points along each otolith contour, maintaining equal distances between these points (n=200). This approach mitigated potential bias arising from different point densities across contours. Each otolith contour was mathematically described by parametric functions $x(\theta)$ and $y(\theta)$ [14], which traced through all points starting from the otolith's rostrum. Elliptical Fourier Descriptors (EFD) were used. We extracted the first 99 elliptical Fourier harmonics (H) for each otolith. These harmonics were normalized to the first harmonic and made invariant to otolith size, rotation, and the starting point of contour description. To determine the optimal number of harmonics needed to reconstruct the otolith outline with à precision of 99%, the cumulated Fourier Power was used [27]. Across all otoliths, we employed a maximum of 33 harmonics (max(nk)) to reconstruct individual otolith contours and perform subsequent 2D analyses. The 3D otolith meshes were standardized to 10,000 triangles with 5,002 vertices per otolith. After this preliminary step, the mean shape for all individuals was rebuilt, and all individual images were aligned from this mean shape. Fourier coefficients were extracted automatically using the SPHARM analysis [4, 27] implemented in R via a custom-coded Matlab function [1]. The meshes were characterized by 35 harmonics (or degree) and 4 icosahedral subdivisions. The surface of each mesh was mathematically described using three parameterized variables: $x(\theta, \phi)$, $y(\theta, \phi)$, and $z(\theta, \phi)$ [28]. Spherical Fourier Descriptors (SFD) were used.

2.4 Shape-based classification

Firstly, Principal Components Analysis (PCA) was applied to the EFD and SFD matrix from 2D and 3D images of otolith. Only a limited number of PCs were used, with 25, 50, 75 and 100 percent of explained variance (figure 3). By reducing dimensionality, only the significant principal components (PCs) were retained.

Unsupervised classifiers. Unsupervised classification methods aim to uncover hidden structures in unlabeled data. In this study, the groups were identified based on their shapes using k prior class information identical with both environmental clusters, other stock proposals and GSAs. So each method requiring the number of clusters is tested for k=[2,3,7,16].
Agglomerative Hierarchical clustering (Ward.d2) [36] was

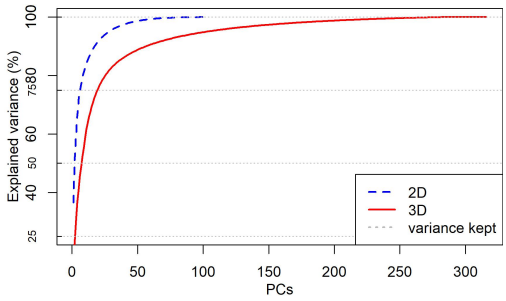

Figure 3: Number of PCs according to the percentage of explained variance for 2D and 3D shape analysis

used to construct a cluster tree by successively merging groups. At the beginning, each data point starts as a singleton cluster, then they are merged iteratively to obtain a unique cluster. This method allows the exploration of different levels of granularity in clustering, and provides a hierarchical representation of the data, enabling the identification of clusters at multiple scales.
K-means [17] was used to partition the data into k clusters by minimizing intra-cluster variance. This method iteratively assigns each data point to the nearest cluster centroid and updates the centroids based on the mean of the data points assigned to each cluster. It is simple, fast, and effective for grouping similar shapes, and works well when clusters are well-separated and roughly spherical.
DBSCAN [11] was used to identify areas of high density and form clusters around them. This method defines clusters as areas of high density separated by areas of low density. An epsilon between 0.025 and 1 was used and the number of minimum points required was 2. This method is robust to non-spherical shapes and can handle noise effectively. It does not require the user to specify the number of clusters in advance and can identify clusters of arbitrary shapes and sizes.
Spectral K-medoid Clustering (Spectral-PAM) [23] was used, also with a recursive version. This method uses the eigenvalues of the Laplacian matrix to cluster the data. It projects the data into a lower-dimensional space using eigenvectors corresponding to the smallest eigenvalues of the Laplacian matrix and then applies K-medoid clustering in the projected space. Spectral Clustering is effective in capturing complex and non-linear structures. It can identify clusters that may not be well-separated or spherical in shape and is particularly useful for data with intricate geometric structures. The first third levels were applied for the spectral recursive version. For each combination of data dimensions, number of PCAs and clustering method, the Adjusted Rand index (ARi) was applied to evaluate the similarity between predicted and other information on the stock structure (GSAs, other stock proposals and environment clusters).

Supervised classifiers. Supervised classification methods use prior learning information to predict classes. In

this case study, information on the stock structure from the expert group (GSAs, other stock proposals) was applied to train the different models. The dataset was split in two equal groups with 50% per GSA of dataset to train the model, and the other 50% to test the model.

Linear Discriminant Analysis (LDA) [12] was used to find a linear combination of features that gave the best boundary to discriminate the classes by maximizing the between-class variance and minimizing the within-class variance. LDA is particularly useful when the classes are linearly separable and assumes that the data are normally distributed within each class. It provides a simple and interpretable solution for classification tasks.

K-Nearest Neighbors (KNN) [47] (with K=[1,3,5,10]) was used to assign a class to a data point based on the majority vote of its k nearest neighbors in the feature space. It calculates the distance between data points to determine similarity. This method is a non-parametric, lazy learning algorithm that does not make any assumptions about the underlying data distribution. It is particularly effective for data with complex decision boundaries and can handle both numerical and categorical data.

Random Forest [5] (number of trees=[10, 50, 100, 200] and split=1) was used to build multiple decision trees during training and combine their predictions through a majority vote to classify. It is an ensemble learning method that is robust to overfitting and noise in the data. It can handle high-dimensional data and interactions between features, making it suitable for a wide range of classification tasks.

Support Vector Machine (SVM) [49] (kernel=[linear,radial,sigmoid]) was used to find the optimal hyperplane that separates classes in the feature space. For linear SVM, it seeks a linear decision boundary, while for Radial Basis Function (RBF), it uses a non-linear decision boundary. RBF SVM can capture complex relationships between features. SVM with different kernel functions, including linear, radial, and sigmoid, was used allowing flexibility in modeling various types of distributions. SVM is effective in high-dimensional spaces and is suitable for both linear and non-linear classification tasks. For each shape data (2D and 3D), principal component count, and chosen supervised classifier technique, we computed accuracy metrics to assess the correspondence between predicted outcomes and various information on the stock structure (such as GSAs, other stock proposals).

3 Results

Unsupervised classifier. From unsupervised classifications, the results were quite similar whether using otolith shape with 2D or 3D images (figure 4). None of the two dimensions (*i.e.* 2D and 3D descriptors) stands out significantly. However, the stock structure seems to be optimised with 2 clusters. In fact, the Adjusted Rand index (ARi) value is higher than other divisions whatever the prior information group (*i.e.* environment clustering or expert groups or GSAs), as shown in figure 4. When using 2D shape analysis, the DBSCAN method appears to have the highest ARi, followed by K-means. In 3D, however, the results are quite similar for most classifiers (figure 4). Depending on the labels used, sometimes DBSCAN stands out slightly. Despite the higher ARi values obtained with DBSCAN, however, a considerable set of the data is unclassified. In most cases, approximately half of the data was classified as noise, with 176±137 and 210±83 of noise, respectively, in 2D and 3D analysis. DBSCAN was, therefore, no longer used for the remainder of the analysis of the results. Furthermore, to streamline the presentation of results, the ARi values were compared to clusters with only 2 stocks, as they exhibited the highest average ARi values, namely 0.36±0.26 and 0.43±0.17, respectively, for 2D and 3D. With all the clustering methods used, increasing the parameter k resulted in higher ARi values (*i.e.* with the

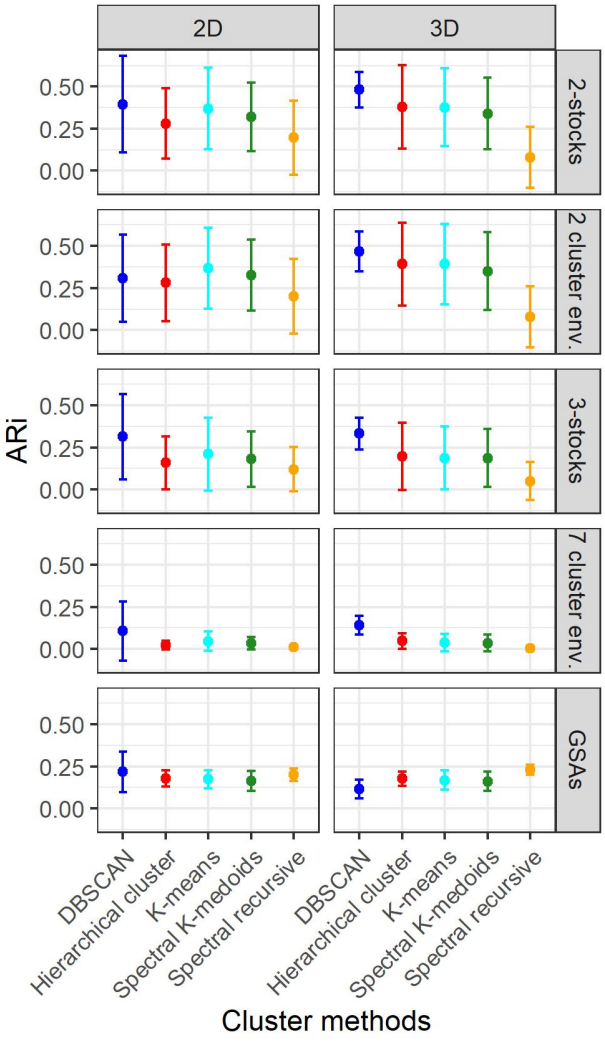

Figure 4: Adjusted Rand index mean and range between prior knowledge and clusters per shape descriptor (2D or 3D) and per clustering method

highest ARi values, which were observed with the highest k values; figure 5). However, the number of PCs did not

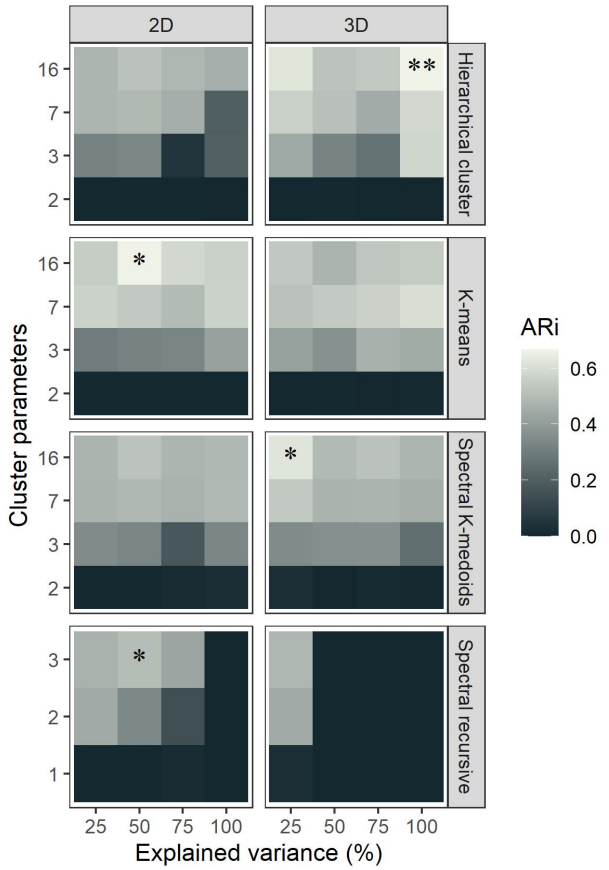

Figure 5: Adjusted Rand index compared by prior 2-stocks division (* represent the highest ARi on the cluster, ** shows the highest ARi among all clustering methods) according to the total explained variance per shape descriptor (2D or 3D) and per clustering method

significantly affect the results, except for the spectral recursive method. The higher the variance with this method, the lower the ARi value (figure 5). To achieve pair matching as close as possible to the prior 2-stocks division (ARi=0.67), the use of 3D otolith shape seemed to be optimal, especially with hierarchical clustering (figure 5). As a secondary option (ARi=0.66), for better classification of the 2D otolith shape, the K-means method was the most relevant. However, even when using the highest ARi value, the predicted clusters did not align with the prior 2-stocks division (figure 6). There was considerable confusion in the predicted clusters across different longitudinal values (as illustrated in figure 6 and other methods and parameters used).

Supervised classifier. Of all the models, KNN with k=1 and all Random Forest (RF) with all ntrees tested performed the best learning rate, achieving an accuracy superior to 99%. In contrast, the other methods exhibited an average accuracy of only 60% (as 3NN). Similarly, among the

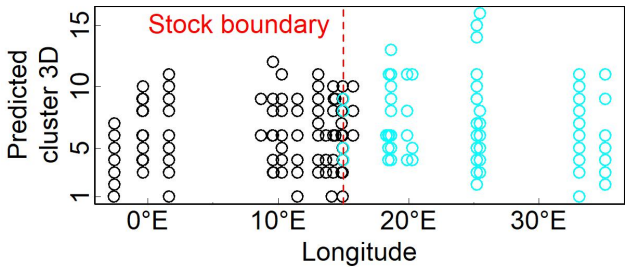

Figure 6: Distribution of individual fish according to the longitude for HC label obtained with K=16-cut. The red line represents the stock boundary. The 2-stocks division are represented by the color (black/cyan).

supervised methods, those employing labels with 2 stocks were the most effective, mirroring the performance seen in the unsupervised methods (figure 7). In the testing set, accuracies of 53±5% and 57±5% were achieved in 2D and 3D, respectively. Notably, the Random Forest (RF) classification method demonstrated distinct characteristics compared to the other methods (figure 7). Furthermore, 3D descriptors showed substantial, positive differences compared to the 2D descriptors (*i.e.* with about 10% gap of successful recognition for RF). This tendency seems to be confirmed for the other methods. When delineating into two stocks, 3D shape analysis consistently demonstrated the highest accuracy irrespective of the classification method employed, except KNN with k=5 and k=10 (figure 8). For several methods, including Random Forest, LDA and all SVMs, increasing the explained variance of the data used resulted in improved model efficiency. Notably, Random Forest with ntree=50 using 3D otolith shape was the most accurate method for delineating stocks into 2 (figure 8). However, even with this improved method, visualizing the stock boundary remains relatively challenging. A significant amount of confusion was still observed when examining the predicted labels (figure 9).

4 Discussions

This study aimed to evaluate the effectiveness of shape analysis dimensions (2D and 3D) and several types of classification for delimiting red mullet stocks in the Mediterranean Sea. With objective (1), the 3D shape analysis of the otoliths yielded results that were relatively similar to those obtained from the 2D analysis during unsupervised classification. However, the 3D analysis consistently exhibited the highest ARi values. Additionally, across all the supervised classification methods tested, the 3D analysis consistently demonstrated superior accuracy compared to the 2D analysis. Therefore, whether employing supervised or unsupervised classifications, 3D analysis of otolith shape emerges as more relevant and efficient than 2D for stock delimitation. Regarding objective (2), in unsupervised classifications, DBSCAN exhibited the highest ARi, but it generated significant noise, undermining the reliability of the

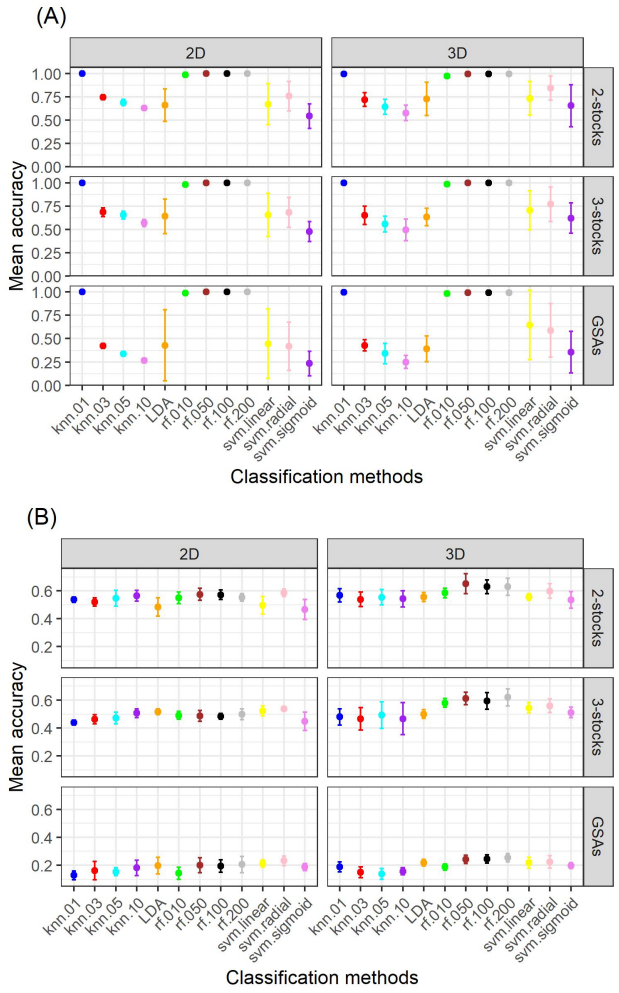

Figure 7: Mean accuracy according to explained variance percent for the training (A) and the testing (B) datasets by shape descriptor (2D or 3D), label comparison, and cluster methods

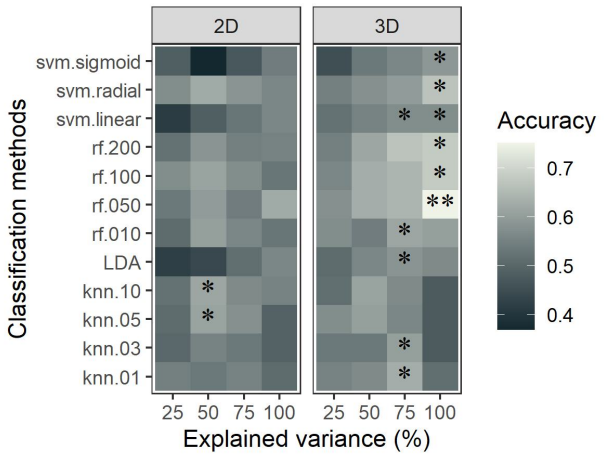

Figure 8: Accuracy of the testing set compared by label with 2 stocks (* represents the highest accuracy on a classification, ** shows the highest accuracy among all methods)

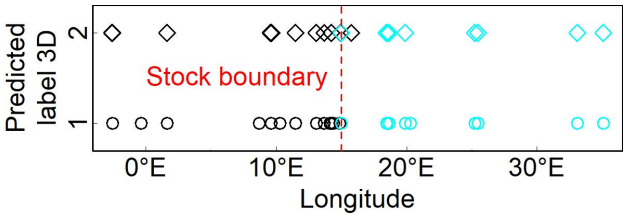

Figure 9: Longitudinal distribution of individual fish according to Random forest with ntrees=50; the red line represents the stock boundary. The 2-stocks division are represented by color (black/cyan).

classification outcomes. This underscores the necessity for robust unsupervised clustering algorithms capable of effectively handling noisy data. Alternatively, hierarchical, K-means, and spectral K-medoids classifications appeared relatively similar, particularly in 3D. Unsupervised classification merely indicated the number of stock divisions present in our samples without revealing their spatial distribution. Despite achieving the highest ARi in tests, locating the spatial division of the 2 stocks was challenging due to considerable confusion among the classifiers. This confusion persisted in supervised classifications; however, they also confirmed the division of stocks into 2. Among the classification methods, Random Forest stood out as the most accurate, particularly when utilising 3D shapes. However, the problem of stock classifications has proved complex, as evidenced by the confusion encountered in identifying the stock boundaries. One hypothesis to consider is that spatial sampling may not have been optimal, which could explain some of the difficulties encountered in stock delineation. It is interesting to note that in supervised classifications, KNN with k=1 showed a higher learning rate than with other k (*i.e.* 3,5,10), suggesting that the model was more sensitive to noise and less robust against atypical samples. Samples closer together may be more effective for classification.

To improve this study, several perspectives could be explored. It is possible that the number of samples used in the study was not sufficient to obtain precise and representative results of the fish population studied. In fact, Random Forest showed overfitting when ntree covered more than 33% of the number of samples. A larger sample size might have led to better coverage of otolith shape variability, resulting in more reliable and generalisable results. Additionally, the distribution of samples by GSAs may have a significant influence on the study's outcomes. Uneven sample distribution among different GSAs could introduce bias into the analysis, as environmental conditions and fish population characteristics may vary from one GSAs to another. Therefore, a balanced distribution of samples by GSAs would be advisable to obtain representative and generalisable results.

Although PCA is commonly used to reduce the dimensionality of data and explore its structure. PCA may struggle to capture nonlinear and complex relationships between variables, leading to significant information loss. In contrast, newer methods like UMAP (Uniform Manifold Approximation and Projection) are designed to capture nonlinear structures and may therefore be a more suitable alternative for exploring otolith shape data [32].

The use of Fourier harmonics for otolith shape analysis has been a commonly employed approach in scientific literature due to its ability to decompose shapes into a series of sinusoidal components. This method has yielded significant results in characterizing otoliths and has contributed to our understanding of their shape and structure. However, it is important to recognize that Fourier analysis may have limitations in capturing all subtle variations in otolith shape [22]. Indeed, it is more suited for representing regular or periodic shapes. For non-periodic or complex shapes, other shape analysis methods may be necessary. Therefore, to further explore the diversity of otolith shapes and improve classification accuracy, it would be beneficial to consider combining Fourier harmonics with other complementary shape descriptors. For example, wavelets or landmark-based descriptors could offer alternative approaches for characterizing complex shapes. Many fishes must migrate for feeding and reproduction. These migrations can result in potential stock overlap [20, 21]. This characteristic makes delineating red mullet stocks particularly challenging, as individuals can move over long distances and interact with different populations. There is a need to develop robust stock delineation methods tailored to this case. This could involve using spatially explicit models and advanced data analysis techniques to account for the dynamics of movement and interactions among red mullet populations. By integrating these considerations into the analysis of red mullet otoliths, it would be possible to enhance the accuracy and reliability of stock delineation methods for this species. However, testing other fish species with different life characteristics (habitats, morphology, diet) could be interesting to test their effect on stock delimitation or on otolith shape.

A promising approach to improve stock delineation would be to conduct multi-tracer analysis, combining data on otolith shape, otolith microchemistry, and fish genetics. Another study has already tested the combination of 2D otolith shape with microchemistry, which showed more effective results compared to shape analysis alone [20]. This integrated approach would gather complementary information on stock structure and provide a more holistic view of fish population variability. Otolith shape data would offer insights into the morphology of otolith structures, allowing for the identification of distinctive features among fish populations. Otolith microchemistry data would provide information about the environment in which the fish lived. This information could be used to reconstruct fish movements and life history. Otolith genetic data would enable the identification of genetic differences among fish populations, providing information on their genetic diversity and genetic structure. This approach would delineate stocks based on their genetic composition and identify populations with high levels of relatedness or genetic differentiation. By combining these different data sources, multi-tracer analysis could compensate for the individual limitations of each method and provide a more comprehensive and accurate picture of stock structure. This integrated approach could assist fishery managers in making more informed decisions regarding conservation and fish stock management, taking into account their genetic diversity, life history, and environment. However, chemical and genetic approaches are time-consuming and expensive. 2D and 3D approaches are easier for data collection and much less costly, but require tools adapted to the small amount of data and their unbalanced distribution.

Acknowledgements. This work has benefited from the grant "ANR-21-EXES-00 11" as part of the IFSEA graduate school (which originates from National Research Agency under the Investments for the Future program), the French Federative Research Structure (SFR Campus de la mer, project No. 2022.7). The otoliths come from the Specific Contract No. 03_EASME/EMFF/2017/1.3.2.3/01/SI2.793201 (MED_UNITs) financed by the European Union. Vinko Bandelj, Fabrizio Gianni and Anna Teruzzi provided the environmental data in the framework of MED-Units Task 4.2. The Sclerochronology team of IFREMER acquired all otoliths 2D images. The authors warmly thank the GISMO platform and its staff (Biogéosciences, University Bourgogne Franche-Comté, UMR CNRS 6282, France) and the team of UMR Transfrontalière BioEcoAgro N○1158, which manages and maintains the analytical equipment used in this study.

References

[1] N. Andrialovanirina et al. "Asymmetry of Sagittal Otolith Shape Based on Inner Ear Side Tested on Mediterranean Red Mullet (Mullus barbatus Linnaeus, 1758): Comparative Analysis of 2D and 3D Otolith Shape Data". In: *Symmetry* 15.5 (May 2023). P. 1067. ISSN: 2073-8994.

[2] G. A. Begg and J. R. Waldman. "An holistic approach to fish stock identification". In: *Fisheries Research* 43.1 (Oct. 1, 1999), pp. 35–44. ISSN: 0165-7836.

[3] I. M. Benson et al. "The future of fish age estimation: deep machine learning coupled with Fourier transform near-infrared spectroscopy of otoliths". In: *Canadian Journal of Fisheries and Aquatic Sciences* 80.9 (Sept. 2023). Pp. 1482–1494. ISSN: 0706-652X.

[4] C. Brechbühler, G. Gerig, and O. Kübler. "Parametrization of Closed Surfaces for 3-D Shape Description". In: *Computer Vision and Image Understanding* 61.2 (Mar. 1, 1995), pp. 154–170. ISSN: 1077-3142.

[5] L. Breiman. "Random Forests". In: *Machine Learning* 45.1 (Oct. 1, 2001), pp. 5–32. ISSN: 1573-0565.

[6] S. Cadrin, L. Kerr, and S. Mariani. *Stock Identification Methods: Applications in Fishery Science: Second Edition*. Elsevier Academic Press, Amsterdam. 2014. 588 pp. ISBN: 978-0-12-397258-3.

[7] S. E. Campana and J. M. Casselman. "Stock Discrimination Using Otolith Shape Analysis". In: *Canadian Journal of Fisheries and Aquatic Sciences* 50.5 (May 1, 1993), pp. 1062–1083. ISSN: 0706-652X, 1205-7533.

[8] L. Cañás et al. "Use of the otolith shape analysis in stock identification of anglerfish (Lophius piscatorius) in the Northeast Atlantic". In: *ICES Journal of Marine Science* 69.2 (Mar. 1, 2012), pp. 250–256. ISSN: 1054-3139.

[9] J. M. Casselman. "Determination of age and growth, In: Weatherley, A.H., Gill, H.S. (Eds.), The Biology of Fish Growth". In: *Determination of age and growth, In: Weatherley, A.H., Gill, H.S. (Eds.), The Biology of Fish Growth*. Academic Press. New York, 1987, pp. 209–242.

[10] R. Escudier et al. "Mediterranean Sea Physical Reanalysis (CMEMS MED-Currents) (Version 1) [Data set: doi.org/10.25423/CMCC/MEDSEA _MULTIYEAR_PHY_006_004_E3R1]". In: *Copernicus Monitoring Environment Marine Service (CMEMS)* (2020).

[11] M. Ester, H-P. Kriegel, and X. Xu. "A Density-Based Algorithm for Discovering Clusters in Large Spatial Databases with Noise". In: *Institute for Computer Science* (1996), p. 6.

[12] R. A. Fisher. "The Use of Multiple Measurements in Taxonomic Problems". In: *Annals of Eugenics* 7.2 (1936). Pp. 179–188. ISSN: 2050-1439.

[13] ICES. "ICES Stock Identification Methods Working Group (SIMWG)". In: 5.101 (2023), p. 153.

[14] F. Kuhl and C. Giardina. "Elliptic Fourier features of a closed contour". In: *Computer Graphics and Image Processing* 18.3 (Mar. 1, 1982), pp. 236–258. ISSN: 0146-664X.

[15] W. Li et al. "Otolith Shape Analysis as a Tool to Identify Two Pacific Saury (Cololabis saira) Groups from a Mixed Stock in the High-Seas Fishing Ground". In: *Journal of Ocean University of China* 20.2 (Apr. 1, 2021), pp. 402–408. ISSN: 1993-5021.

[16] L. A. Libungan and S. Pálsson. "ShapeR: An R Package to Study Otolith Shape Variation among Fish Populations". In: *PLOS ONE* 10.3 (Mar. 24, 2015). e0121102. ISSN: 1932-6203.

[17] S. P. Lloyd. "Least squares quantization in PCM". In: *Technical Report RR-5497, Bell Lab* (Sept. 1957).

[18] J. J. I. Mapp et al. "Three-dimensional rendering of otolith growth using phase contrast synchrotron tomography". In: *Journal of Fish Biology* 88.5 (2016). Pp. 2075–2080. ISSN: 1095-8649.

[19] P. Marti-Puig et al. "New parameterisation method for three-dimensional otolith surface images". In: *Marine and Freshwater Research* 67.7 (2016), p. 1059. ISSN: 1323-1650.

[20] B. Morales-Nin et al. "European hake (Merluccius merluccius) stock structure in the Mediterranean as assessed by otolith shape and microchemistry". In: *Fisheries Research* 254 (Oct. 1, 2022), p. 106419. ISSN: 0165-7836.

[21] F. Morat et al. "Discrimination of red mullet populations (Teleostean, Mullidae) along multi-spatial and ontogenetic scales within the Mediterranean basin on the basis of otolith shape analysis". In: *Aquatic Living Resources* 25.1 (Jan. 2012), pp. 27–39. ISSN: 0990-7440, 1765-2952.

[22] J. Neves et al. "Comparing otolith shape descriptors for population structure inferences in a small pelagic fish, the European sardine Sardina pilchardus (Walbaum, 1792)". In: *Journal of Fish Biology* 102.5 (May 2023), pp. 1219–1236. ISSN: 1095-8649.

[23] A.Y. Ng, M.I. Jordan, and Y. Weiss. "On Spectral Clustering: Analysis and an algorithm." In: *NIPS*. Ed. by Thomas G. Dietterich, Suzanna Becker, and Zoubin Ghahramani. MIT Press, 2001, pp. 849–856.

[24] V. Parisi-Baradad et al. "Otolith shape contour analysis using affine transformation invariant wavelet transforms and curvature scale space representation". In: *Marine and Freshwater Research* 56.5 (2005), p. 795. ISSN: 1323-1650.

[25] M. J. Quindazzi, A. Summers, and F. Juanes. "Efficiency is doing things right: high-throughput, automated, 3D methods in the modern era of otolith morphometrics". In: *Canadian Journal of Fisheries and Aquatic Sciences* 79 (2022), p. 7.

[26] T. Schulz-Mirbach et al. "Auditory chain reaction: Effects of sound pressure and particle motion on auditory structures in fishes". In: *PLOS ONE* 15.3 (Mar. 27, 2020). e0230578. ISSN: 1932-6203.

[27] L. Shen, H. Farid, and M. McPeek. "Modeling three-dimensional morphological structures using spherical harmonics". In: *Evolution* 63.4 (Apr. 2009), pp. 1003–1016. ISSN: 00143820, 15585646.

[28] L. Shen and F. Makedon. “Spherical mapping for processing of 3D closed surfaces”. In: *Image and Vision Computing* 24.7 (July 1, 2006), pp. 743–761. ISSN: 0262-8856.

[29] K. Sherman et al. “A global movement toward an ecosystem approach to management of marine resources”. In: *Marine Ecology Progress Series* 300 (2005). Pp. 275–279. ISSN: 0171-8630.

[30] M. T. Spedicato et al. “Spatial distribution of marine macro-litter on the seafloor in the northern Mediterranean Sea: the MEDITS initiative”. In: *Scientia Marina* 83 (Dec. 1, 2019).

[31] A. Teruzzi et al. “Mediterranean Sea Biogeochemical Reanalysis (CMEMS MED-Biogeochemistry, MedBFM3 system) (Version 1) [Data set: doi.org/10.25423/CMCC/MEDSEA_MULTIYEAR_BGC_006_008_MEDBFM3]”. In: *Copernicus Monitoring Environment Marine Service (CMEMS)* (2021).

[32] K. Al-Thelaya et al. “InShaDe: Invariant Shape Descriptors for visual 2D and 3D cellular and nuclear shape analysis and classification”. In: *Computers & Graphics* 98 (Aug. 1, 2021), pp. 105–125. ISSN: 0097-8493.

[33] V. Tuset et al. “Paradox of otolith shape indices: routine but overestimated use”. In: *Canadian Journal of Fisheries and Aquatic Sciences* 78.6 (June 2021). Pp. 681–692. ISSN: 0706-652X.

[34] J. Vasconcelos-Filho et al. “Peeling the Otolith of Fish: Optimal Parameterization for Micro-CT Scanning”. In: *Frontiers in Marine Science* 6 (2019). ISSN: 2296-7745.

[35] M. Vignon. “Disentangling and quantifying sources of otolith shape variation across multiple scales using a new hierarchical partitioning approach”. In: *Marine Ecology Progress Series* 534 (Aug. 27, 2015), pp. 163–177. ISSN: 0171-8630, 1616-1599.

[36] J. H. Ward Jr. “Hierarchical Grouping to Optimize an Objective Function”. In: *Journal of the American Statistical Association* 58.301 (Mar. 1, 1963). Pp. 236–244. ISSN: 0162-1459.

[37] C. Wei and R. McCauley. “Numerical modeling of the impacts of acoustic stimulus on fish otoliths from two directions”. In: *The Journal of the Acoustical Society of America* 152.6 (Dec. 2022). Pp. 3226–3234. ISSN: 0001-4966.

[38] C. Zhang et al. “Population structure of Japanese Spanish mackerel Scomberomorus niphonius in the Bohai Sea, the Yellow Sea and the East China Sea: evidence from random forests based on otolith features”. In: *Fisheries Science* 82.2 (Mar. 1, 2016), pp. 251–256. ISSN: 1444-2906.

[39] L. Zhuang, Z. Ye, and C. Zhang. “Application of otolith shape analysis to species separation in Sebastes spp. from the Bohai Sea and the Yellow Sea, northwest Pacific”. In: *Environmental Biology of Fishes* 98.2 (Feb. 1, 2015), pp. 547–558. ISSN: 1573-5133.

[40] A. Zitek et al. “Affordable 3D scanning of small otoliths for improved shape analysis by photogrammetry techniques”. In: 5th International Otolith Symposium 2014 (IOS2014). Mallorca, Spain, Oct. 22, 2014.